THE JOURNAL OF PHYSICAL CHEMISTRY Letters

Letter

pubs.acs.org/JPCL

Determination of Excited-State Energies and Dynamics in the B Band of the Bacterial Reaction Center with 2D Electronic Spectroscopy

Gabriela S. Schlau-Cohen,[†,§,⊥] Eleonora De Re,[‡,§] Richard J. Cogdell,[∥] and Graham R. Fleming*[,†,‡,§]

[†]Department of Chemistry and [‡]Graduate Group in Applied Science and Technology, University of California − Berkeley, Berkeley, California, United States

[§]Physical Biosciences Division, Lawrence Berkeley National Lab, Berkeley, California, United States

[∥]University of Glasgow, Glasgow, United Kingdom

Supporting Information

ABSTRACT: Photosynthetic organisms convert photoenergy to chemical energy with near-unity quantum efficiency. This occurs through charge transfer in the reaction center, which consists of two branches of pigments. In bacteria, both branches are energy-transfer pathways, but only one is also an electron transfer pathway. One barrier to a full understanding of the asymmetry is that the two branches contain excited states close in energy that produce overlapping spectroscopic peaks. We apply polarization-dependent, 2D electronic spectroscopy to the B band of the oxidized bacterial reaction center. The spectra reveal two previously unresolved peaks, corresponding to excited states localized on each of the two branches. Furthermore, a previously unknown interaction between these two states is observed on a time scale of ∼100 fs. This may indicate an alternative pathway to electron transfer for the oxidized reaction center and thus may be a mechanism to prevent energy from becoming trapped in local minima.

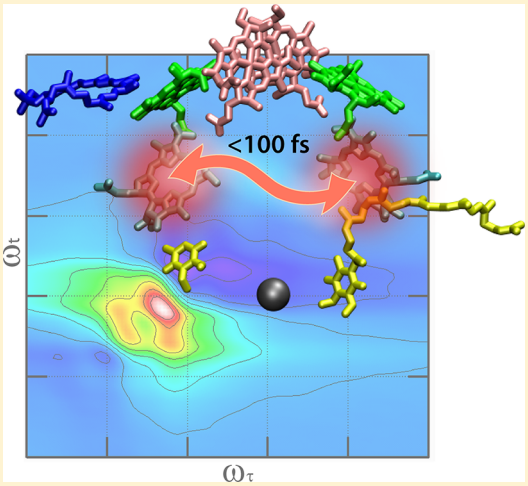

SECTION: Biophysical Chemistry and Biomolecules

In photosynthesis, absorbed sunlight is converted to chemical energy with near-unity quantum efficiency.[1,2] After absorption, which occurs primarily in the antenna complexes in the outer regions of the photosynthetic apparatus, the excitation energy is transferred to a central location, the reaction center. In the reaction center, an initial charge separation event occurs, which initiates a subsequent chain of electron-transfer reactions.[3,4] The antenna complexes and the reaction center are pigment protein complexes (PPCs), which consist of densely packed pigments surrounded by a protein matrix. Although antenna complexes exhibit a large amount of architectural and size diversity,[5−8] the molecular structure of the reaction center is highly conserved across species.[9] The bacterial reaction center (bRC) is an ideal model system for studying the functionality of reaction centers because it has been extraordinarily well-characterized by numerous spectroscopic techniques, biochemical experiments, and structural studies.[1,4] The bRC consists of two branches of chromophores, called A and B, that are arranged with pseudo-C_{2v} symmetry (shown in Figure 1a). Each branch contains two bacteriochlorophylls (BChl), a bacteriopheophytin (BPheo), and a quinone (Q), with a carotenoid found next to the B branch.[1,9,10] The linear absorption spectrum, shown in Figure 1b, exhibits a series of well-separated peaks. Most of these peaks contain two states, one from each of the two branches. The two branches are structurally similar, and both serve as efficient energy-transfer pathways, meaning the excitation moves up the branches to the two BChls known as the special pair (labeled as P in Figure 1a), where charge separation is usually initiated. Strong pigment−pigment interactions, which have been predicted theoretically and observed experimentally, give rise to these energy-transfer processes.[11,12] Upon charge separation, however, electron transfer occurs only down the A branch to Q_A.[13,14] From Q_A, the electron transfers to Q_B, after which, when Q_B is fully reduced, it leaves its binding pocket to drive downstream biochemistry.[3] Extensive investigations into the structure, biochemistry, and photophysics of the bRC[15−19] have examined the differences in protein environment and the resultant functional asymmetry. Despite this effort, the differences in excited-state energies and dynamics remain incompletely described.

Two-dimensional electronic spectroscopy maps the electronic structure and dynamics of condensed phase systems.[20−22] Two-dimensional spectra are frequency−frequency

Received: June 28, 2012
Accepted: August 13, 2012

   dx.doi.org/10.1021/jz300841u | J. Phys. Chem. Lett. 2012, 3, 2487−2492

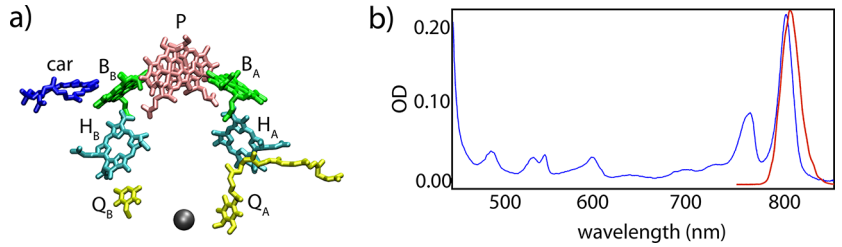

Figure 1. Structural model and linear absorption of the bacterial reaction center. (a) Structure of the bacterial reaction center from *Rb. sphaeroides* as determined by X-ray crystallography (PDB code: 2J8C). For clarity, the phytol tails of all bacteriochlorins are truncated. The two branches of pigments both transfer photoenergy to the special pair, P. Upon charge separation, electrons transfer down the A branch. (b) Linear absorption spectrum of the oxidized bacterial reaction center from Ga-strain *Rb. sphaeroides* at 77 K. The excitation laser spectrum is shown as the red line.

correlation plots, where the dependence of emission energy on excitation energy is represented for a selected set of time delays between excitation and emission events. These plots display excited-state energies, excited-state couplings, and energy transfer with femtosecond time resolution.[23] From the resultant enhanced spectral resolution across both the excitation and emission axes, this technique can reveal features that are buried in other linear and nonlinear spectroscopies.[24] In particular, the antidiagonal elongation in the nonrephasing component of 2D spectra provides a means to separate closely spaced excited states.[25]

Here we describe 2D experiments on the B band of the oxidized bRC (the peak at ~800 nm or 12 500 cm^{-1}, in Figure 1b, arising from the BChl labeled as B_A and B_B in Figure 1a). Under high light conditions, a large percentage of the reaction centers are oxidized (closed), and if left unquenched, excited BChl can convert to a triplet state, which can generate deleterious reactive oxygen species. Regenerating the reaction center carries both metabolic (production of new pigments) and opportunity (lost charge separation events during regenerative time) costs. Understanding the dynamics in the oxidized bRC can reveal how it is protected in the absence of the electron transfer pathway. We have investigated the two states proximal to the site of charge separation, the Q_y ($S_0 \rightarrow S_1$) transitions of B_A and B_B, which correspond to the final steps in the energy transfer chain before the excitation reaches the oxidized special pair. These two states appear as a single peak in linear and nonlinear spectra, which has obscured efforts to investigate their separate dynamics. Spectroscopic studies have, however, indirectly indicated differences in the energies of B_A and B_B. Three-pulse photon echo peak shift (3PEPS) experiments observed two separate bath correlation time scales within the B band of 60 and 90 fs determined under 790 and 810 nm excitation, respectively.[26] Additionally, results from transient absorption experiments with both oxidized and neutral bRCs suggested that, after excitation of the B band, energy transfer along the A branch is slightly faster.[27−29] Finally, transient absorption spectra suggest an alternate charge-separation pathway, with an initial state of $B_A^+H_A^-$, that forms only along the A branch. As this charge-separated state has been observed primarily in the H_x region, this branch-specific effect will fall outside the spectral window of the experimental results discussed in this work.[30] Here we exploit the spectral resolution in excitation and emission provided by 2D spectroscopy as well as the antidiagonal elongation seen in nonrephasing 2D spectra to achieve direct observation of two separate excited-state energies for the first time and relaxation dynamics for the two states within the B band.

Two-dimensional real, nonrephasing spectra of the Q_y region are shown in Figure 2. In the linear absorption spectrum shown

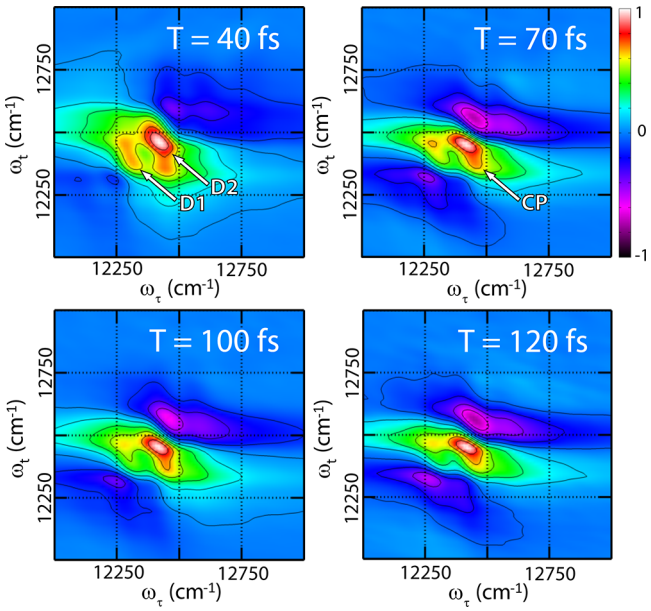

Figure 2. Real, nonrephasing 2D spectra of the B band at selected waiting times at 77 K taken under the all-parallel polarization. Each spectrum is normalized to its own maximum. These spectra exhibit two separated states along the diagonal, labeled D1 and D2 in the T = 40 fs spectrum. Energy transfer between these two states appears in the increase in intensity of the cross-peak labeled CP in the T = 70 fs spectrum. The T = 100 and 120 fs begin to show energy transferring out of band, first from D1.

in Figure 1b, the two B-band states appear as one peak centered close to 800 nm (12 500 cm^{-1}). In the nonrephasing component of the 2D spectra, two distinct excited states and the dynamics of these two states can be observed. As labeled in the T = 40 fs spectrum, the 2D nonrephasing spectra exhibit two separate positive, diagonal peaks, corresponding to the two states in the B band that are labeled D1 (12 325 cm^{-1}) and D2 (12 450 cm^{-1}). The B-band peak observed in the 2D nonrephasing spectra is slightly red-shifted from the linear absorption peak due to the partial overlap with the negative, excited-state absorption (ESA) feature at ~12 550 cm^{-1}. A second, less intense ESA peak lies at lower energy (~12 200 cm^{-1}). The ESA peaks increase in intensity relative to the positive diagonal peaks until ~50 fs and then show near-constant intensities relative to the positive diagonal features through the 150 fs waiting time, which is the time window

dx.doi.org/10.1021/jz300841u | *J. Phys. Chem. Lett.* 2012, 3, 2487−2492

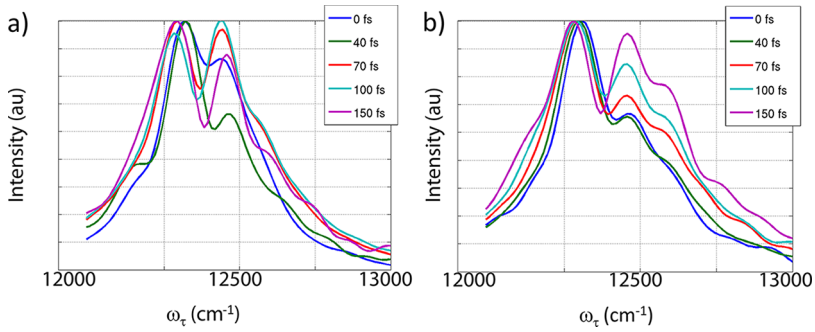

Figure 3. Normalized, horizontal slices from the absolute value, nonrephasing 2D spectra at ω_t = 12 325 cm^{-1} for (a) all-parallel and (b) cross-peak-specific polarization sequences. The difference in scaling with polarization, as appears in the clear grow-in of the cross-peak (ω_τ = 12 450 cm^{-1}) under the cross-peak-specific sequence, indicates the existence of an energy-transfer pathway. The suppression of other features also allows the appearance at 70 fs and relative increase in the cross-peak to be more clearly observed.

discussed here. On the basis of previous assignments, D1 most likely corresponds to the B_B transition, and D2 most likely corresponds to the B_A transition.[26,30] Using polarized linear absorption on neutral bRC crystals, the excited-state energies were determined to be 800 nm (12 500 cm^{-1}) for B_A and 810 nm (12 345 cm^{-1}) for B_B, which compare favorably to our values of 12 450 and 12 325 cm^{-1}.[30] The small shifts may be from the ESA peaks that contribute to nonlinear spectra or from the change in local environment due to formation of P^+. Energy transfers out of the B band (to states localized on P^+) by the T = 300 fs spectrum (not shown). This is also in accordance with previous results, in this case transient absorption measurements.[27] As energy transfers out of D1 and D2, the positive signal from stimulated emission decreases and so cancels out less and less of the negative ESA, resulting in an increase in relative intensity of both negative peaks. However, a second notable feature from the separation of the two peaks is that, as seen in the T = 120 fs spectrum in Figure 2, energy transfers out of the D1 state at a slightly faster rate than out of D2.

In the early time spectra (<100 fs), population moving between these two states can be observed by the presence of cross-peaks connecting these two transitions. (The below-diagonal peak is labeled as CP in the T = 70 fs spectrum.) There are cross-peaks above and below the diagonal, indicating population transfer in both directions between the two states in the B band. The maximum intensity of CP occurs at T = ∼70 fs, as population then transfers out of band with a similar time scale as D1. Two distinct transitions as well as interactions between them were not previously observed with other techniques.

The polarization dependence of CP provides further evidence of energy transfer and a greater ability to quantify energy transfer.[31] We investigate the cross-peak below the diagonal. Within a 2D spectrum, each peak is scaled by an orientational prefactor based on the angles between the transition dipole moments in the molecular frame and the angles between the laser pulse polarizations in the lab frame. This has been extensively described elsewhere.[24,31−33] Except in the case of energy transfer between a donor and acceptor with parallel transition dipole moments, cross-peaks will scale differently with changes to the polarization of the incident beams than will diagonal peaks corresponding to absorption and emission from the same state. Spectra were recorded under the all-parallel (0,0,0,0) and cross-peak-specific (π/3,−π/3,0,0) polarization sequences, which are polarization sequences that maximize intensities for energy-transfer steps between parallel transitions and between perpendicular transitions, respectively. We refer to the latter as the cross-peak-specific sequence. Absolute value, nonrephasing spectra taken under the cross-peak-specific polarization sequence are shown in the Supporting Information. The change in scaling of energy-transfer peaks relative to diagonal peaks under these two polarization sequences has been described in detail in previous work.[24,34]

Horizontal slices at the emission energy of D1 (12 325 cm^{-1}) are shown in Figure 3 for both the parallel and cross-peak-specific polarization sequences. CP contains intensity from both energy transfer and the dispersive tails of the diagonal peaks. In the all-parallel slices, there are similar relative amplitudes of CP and D1, and compression and spectral fluctuations produce the small intensity fluctuations as a function of waiting time. Under the cross-peak-specific polarization, however, the suppression of the diagonal peaks also suppresses the dispersive tails. This allows a relative enhancement of energy-transfer peaks, and the energy-transfer step appears much more clearly. Specifically, there is a clear increase in relative intensity as amplitude moves from D1 to D2, or as the cross-peak grows in, as shown in Figure 3b. The CP increases in relative intensity between 40 and 150 fs. This strongly suggests that energy transfer occurs in ∼100 fs. If there was no population transfer between these two states, then the difference in polarization sequence would not change the relative intensities of the two peaks. These spectra provide, for the first time, direct evidence of interaction between the two states within the B band.

Whereas the spectra show that amplitude initially on one state in the B band ends up localized on the other, the underlying mechanism remains unknown. There are several possibilities, which we will now discuss, along with an evaluation of their probability. The simplest possibility is that energy could transfer directly from B_A to B_B. On the basis of the calculated B_A to B_B coupling (J = 45 cm^{-1}),[35] the energy gap between the two excited states (125 cm^{-1}), and the reorganization energy due to electron−phonon coupling (80 cm^{-1}), an energy-transfer time scale of a few hundred femtoseconds would be expected. This determination of a rough time scale was made by comparison to the extensive theoretical modeling of each energy-transfer step in the Fenna−Matthews−Olson (FMO) complex.[36] Therefore, the sub-100 fs time scale observed experimentally most probably does not arise from standard energy transfer between the two states.

The second possibility is some component of the energy transfers before localization occurs. The energy eigenstates, or

dx.doi.org/10.1021/jz300841u | J. Phys. Chem. Lett. 2012, 3, 2487−2492

excitons, are delocalized excited states constructed from linear combinations of the excited states of the individual BChl. Calculations on the oxidized bRC have produced the two excitons localized primarily on the B band. The major site basis contributions to these two states are 0.52 and 0.15 from B_A, 0.21 and 0.74 from B_B, and 0.16 and 0.06 from P_S^+ (one of the states localized on the oxidized special pair).[35] Therefore, these two eigenstates, which are the initially excited states, both have contributions from B_A, B_B, and P^+. Previous experimental and theoretical work has shown that energy transfer can occur rapidly (~100 fs) in the event of spatial overlap between excitons. Energy-transfer rates are determined by a balance of electronic coupling and electron−phonon coupling, which is coupling to the protein bath.[37,38] When the electron−phonon coupling is greater than the electronic coupling, the excitation localizes and energy transfer occurs via hopping from one state to another. There is a time scale associated with localization as phonon reorganization dynamics take place after excitation or re-equilibration of the nuclei in response to the electronic excitation. Before localization, some component of the population can exploit the spatial overlap of these two excitons and transfer rapidly between them.

A third possibility is that the population transfers via two individual energy-transfer steps. Theoretical results have shown several weakly optically allowed states localized on P^+, the oxidized special pair, that have energies close to the B band.[35] Therefore, energy can transfer from B_A first to these states on P^+, and then to B_B. In the case of two sequential incoherent energy transfer steps, the first step (B_A to P^+) is 200 fs. The second step is longer because although the P^+ to B_B rate cannot be directly measured, the B_B to P^+ rate, which should be faster because it is a downhill transfer, is 400 fs.[29] These two time scales make it unlikely that a component would be visible via this pathway in <100 fs.

The fourth possibility is that there is a coherent sequence of B_A de-excitation, P^+ excitation and de-excitation, and finally B_B excitation. With this sequence, the rate can increase[39,40] according to a superexchange or a "through bond" mechanism, where a linker can mediate indirect coupling between two states. Energy transfer from B_A to B_B can be mediated by these P^+ states serving as a bridge.[41] Experimental and theoretical work has shown that superexchange can produce drastic increases in energy and electron transfer rates.[39−41]

At this point, there is no direct experimental tool to determine whether superexchange or direct energy transfer gives rise to the observed peak. Regardless of mechanism, the experimental results suggest that there is more interaction between the two branches than is often included in the general description of two isolated energy transfer pathways.

The transfer of amplitude from B_A to B_B observed here could offer insight into how the reaction center prevents photodamage by using these states as an alternative pathway for excitation energy. Additionally, this transfer pathway does not interfere with the major dissipation mechanism, whereby the oxidized special pair quenches excitation energy. Photosynthetic systems, however, have multiple levels of safeguards to protect themselves against damage. Whereas there are mechanisms for dissipating harmful photoproducts, such as carotenoids dissipating $BChl^T$ states,[42,43] the energy-transfer pathways are designed to minimize the initial formation of these photoproducts. One mechanism by which this is accomplished is by ensuring that the excitation does not remain trapped in local minima. Experimental and theoretical results show that in purple bacteria around 20% of photoenergy that reaches the bRC is detrapped from the bRC.[44−47] Calculations suggest that only 13% of the detrapped photoenergy is retrapped by the same bRC. Instead, the vast majority migrates to other bRCs.[47] The pathway observed here may aid in preventing the accumulation of photoproducts because the excitation does not remain trapped on a single BChl but can move around the bRC. Either of the BChl could be better positioned for the excitation to transfer back to LH1, depending on PPC to PPC variation in site basis contributions, energies, and transition dipole moments of the low-energy excited states due to protein fluctuations. From LH1, the excitation can then transfer to neighboring antenna and bRCs.

By exploiting the antidiagonal elongation of 2D nonrephasing spectra, the energies of the two distinct, previously inseparable states within the B band were determined, and transfer of amplitude most simply described as energy transfer between these two states was observed for the first time. Furthermore, the energy-transfer process was characterized by comparing results taken under the all-parallel and cross-peak-specific polarization sequences. The observation of a second energy-transfer pathway may inform on how excitations can easily migrate around the photosynthetic apparatus, thus preventing the formation of deleterious photoproducts. The observation of two separated excited states directly displays the difference in electronic structure of the two branches and thus provides a much more direct reporter of difference in the effective molecular structure of the two branches. The observed excited-state energies and dynamics can benchmark microscopic modeling of how small differences in molecular structure, that is, differences between the two branches, give rise to tuned pigment−pigment or pigment−protein couplings. Overall, these results illustrate the wealth of information provided by the addition of spectral resolution along both excitation and emission axes provided by 2D spectroscopy and the potential to access previously unknown dynamics through the extension of the technique into polarized pulse sequences.

EXPERIMENTAL METHODS

Previously described methods were followed in preparing and isolating the reaction centers of *Rhodobacter sphaeroides*, strain Ga.[48] The samples were suspended in 20 mM Tris HCl and 0.1% LDAO buffer (pH 8.0), and 100 mM $K_3Fe(CN)_6$ was added to the buffer to oxidize the primary electron donor, P. The sample was diluted 30:70 (v/v) with glycerol and cooled to 77 K. The OD at 800 nm was 0.2 to 0.3 per 200 μm.

A home-built Ti:sapphire regenerative amplifier, seeded by a home-built Ti:sapphire oscillator, produces a 3.4 kHz pulse train of 45 fs pulses centered at 805 nm with 27 nm of bandwidth, as measured by SHG-FROG.[49] The energy on the sample from each of beams 1, 2, and 3 was 4 nJ per pulse, and beam 4 was attenuated by four orders of magnitude. The beams were focused to a 70 μm beam waist. For the polarization experiments, true zero-order waveplates (CVI) were inserted into beams 1 and 2 and set with a precision of ±2°. All measurements were performed at 77 K.

The details of the experimental apparatus, data acquisition, and analysis have been described in detail elsewhere.[49] The laser beam is split into four beams using a beamsplitter and a diffractive optic. The use of the diffractive optic allows for phase stability between pulse pairs. The four ultrafast beams are incident on the sample in a box geometry. The interaction of three of the beams with the sample generates the signal,

emitted in the phase-matched direction, $\mathbf{k}_s = -\mathbf{k}_1 + \mathbf{k}_2 + \mathbf{k}_3$, collinear with the fourth beam, a local oscillator pulse. The local oscillator is attenuated by four orders of magnitude to ensure that it does not interact strongly with the sample. Using spectral interferometry, the signal is heterodyne-detected in the frequency domain.[50]

The measured electric field is a function of the three time delays between the pulses.[23,51] The time delay between the first two pulses is known as the coherence time, τ, and is controlled to interferometric precision with movable glass wedges, which were scanned from −390 to 390 fs in 1.3 fs steps. Negative coherence times generate the nonrephasing signal, and positive coherence times generate the rephasing signal. Between the second and third pulses, the system evolves dynamically during a so-called "waiting time," T. The third time delay, between pulse 3 and the signal emission, is the rephasing time, t. The frequency−frequency 2D spectrum at fixed T is produced by spectrally resolving the signal along ω_t and then Fourier-transforming along the scanned coherence time axis, τ. In this frequency domain representation, the spectrum directly correlates excitation and emission energies. The ensemble of PPCs evolves in a coherence during both the coherence time and the rephasing time. If the system progresses in conjugate frequencies during these two time periods, then this allows for the reversal of dephasing and the generation of a photon echo signal. To produce a nonrephasing signal, the ensemble of PPCs evolves with a phase factor of the same sign during the coherence time and the rephasing time, thus generating a free induction decay signal. The rephasing and nonrephasing signals are separated experimentally by the time ordering of pulses one and two. The signal generated over the entire scan, or the sum of the photon echo and free induction decay contributions, produces a relaxation spectrum for $T > 0$. Phasing was performed using the projection-slice theorem by separately measuring the spectrally resolved pump−probe signal for each waiting time.[23]

■ ASSOCIATED CONTENT

Supporting Information

Absolute value, nonrephasing 2D spectra taken under the coherence-specific polarization sequence. This material is available free of charge via the Internet at http://pubs.acs.org.

■ AUTHOR INFORMATION

Present Address

[⊥]Department of Chemistry, Stanford University, Stanford, California, United States.

Notes

The authors declare no competing financial interest.

■ ACKNOWLEDGMENTS

This work was supported by the Director, Office of Science, Office of Basic Energy Sciences, of the U.S. Department of Energy under contract DE-AC02-05CH11231 and the Division of Chemical Sciences, Geosciences, and Biosciences, Office of Basic Energy Sciences of the U.S. Department of Energy through grant DE-AC03-76SF000098 (at LBNL and UC Berkeley). G.S.S.-C. thanks the A.A.U.W. American Fellowship for support. R.J.C. thanks the BBSRC for financial support. We thank A. Ishizaki for helpful discussion and A. K. De for experimental assistance.

■ REFERENCES

(1) Blankenship, R. E. *Molecular Mechanisms of Photosynthesis*; Blackwell Science: Oxford, U.K., 2002.
(2) Wraight, C. A.; Clayton, R. K. Absolute Quantum Efficiency of Bacteriochlorophyll Photooxidation in Reaction Centers of Rhodopseudomonas-Spheroides. *Biochim. Biophys. Acta* **1974**, *333*, 246−260.
(3) Zinth, W.; Wachtveitl, J. The First Picoseconds in Bacterial Photosynthesis - Ultrafast Electron Transfer for the Efficient Conversion of Light Energy. *ChemPhysChem* **2005**, *6*, 871−880.
(4) Cogdell, R. J.; Gall, A.; Kohler, J. The Architecture and Function of the Light-Harvesting Apparatus of Purple Bacteria: From Single Molecules to in Vivo Membranes. *Q. Rev. Biophys.* **2006**, *39*, 227−324.
(5) van Amerongen, H.; Valkunas, L.; van Grondelle, R. *Photosynthetic Excitons*; World Scientific: Singapore, 2000.
(6) Fleming, G. R.; Schlau-Cohen, G. S.; Amarnath, K.; Zaks, J. Design Principles of Photosynthetic Light-Harvesting. *Faraday Discuss.* **2012**, *155*, 27−41.
(7) Liu, Z. F.; Yan, H. C.; Wang, K. B.; Kuang, T. Y.; Zhang, J. P.; Gui, L. L.; An, X. M.; Chang, W. R. Crystal Structure of Spinach Major Light-Harvesting Complex at 2.72 Angstrom Resolution. *Nature* **2004**, *428*, 287−292.
(8) Mcdermott, G.; Prince, S. M.; Freer, A. A.; Hawthornthwaitelawless, A. M.; Papiz, M. Z.; Cogdell, R. J.; Isaacs, N. W. Crystal-Structure of an Integral Membrane Light-Harvesting Complex from Photosynthetic Bacteria. *Nature* **1995**, *374*, 517−521.
(9) Ermler, U.; Fritzsch, G.; Buchanan, S. K.; Michel, H. Structure of the Photosynthetic Reaction-Center from Rhodobacter-Sphaeroides at 2.65-Angstrom Resolution - Cofactors and Protein-Cofactor Interactions. *Structure* **1994**, *2*, 925−936.
(10) Roszak, A. W.; McKendrick, K.; Gardiner, A. T.; Mitchell, I. A.; Isaacs, N. W.; Cogdell, R. J.; Hashimoto, H.; Frank, H. A. Protein Regulation of Carotenoid Binding: Gatekeeper and Locking Amino Acid Residues in Reaction Centers of Rhodobacter sphaeroides. *Structure* **2004**, *12*, 765−773.
(11) Lee, H.; Cheng, Y.-C.; Fleming, G. R. Coherence Dynamics in Photosynthesis: Protein Protection of Excitonic Coherence. *Science* **2007**, *316*, 1462−1465.
(12) Parkinson, D. Y.; Lee, H.; Fleming, G. R. Measuring Electronic Coupling in the Reaction Center of Purple Photosynthetic Bacteria by Two-Color, Three-Pulse Photon Echo Peak Shift Spectroscopy. *J. Phys. Chem. B* **2007**, *111*, 7449−7456.
(13) Kirmaier, C.; Holten, D.; Parson, W. W. Temperature and Detection-Wavelength Dependence of the Picosecond Electron-Transfer Kinetics Measured in Rhodopseudomonas-Sphaeroides Reaction Centers - Resolution of New Spectral and Kinetic Components in the Primary Charge-Separation Process. *Biochim. Biophys. Acta* **1985**, *810*, 33−48.
(14) Kirmaier, C.; Holten, D.; Parson, W. W. Picosecond-Photodichroism Studies of the Transient States in Rhodopseudomonas-Sphaeroides Reaction Centers at 5-K - Effects of Electron-Transfer on the 6 Bacteriochlorin Pigments. *Biochim. Biophys. Acta* **1985**, *810*, 49−61.
(15) Heller, B. A.; Holten, D.; Kirmaier, C. Control of Electron-Transfer between the L-Side and M-Side of Photosynthetic Reaction Centers. *Science* **1995**, *269*, 940−945.
(16) Chuang, J. I.; Boxer, S. G.; Holten, D.; Kirmaier, C. High Yield of M-Side Electron Transfer in Mutants of Rhodobacter Capsulatus Reaction Centers Lacking the L-Side Bacteriopheophytin. *Biochemistry* **2006**, *45*, 3845−3851.
(17) Wakeham, M. C.; Jones, M. R. Rewiring Photosynthesis: Engineering Wrong-Way Electron Transfer in the Purple Bacterial Reaction Centre. *Biochem. Soc. Trans.* **2005**, *33*, 851−857.
(18) Stanley, R. J.; King, B.; Boxer, S. G. Excited State Energy Transfer Pathways in Photosynthetic Reaction Centers 0.1. Structural Symmetry Effects. *J. Phys. Chem.* **1996**, *100*, 12052−12059.
(19) Jackson, J. A.; Lin, S.; Taguchi, A. K. W.; Williams, J. C.; Allen, J. P.; Woodbury, N. W. Energy Transfer in Rhodobacter Sphaeroides Reaction Centers with the Initial Electron Donor Oxidized or Missing. *J. Phys. Chem. B* **1997**, *101*, 5747−5754.

(20) Ginsberg, N. S.; Cheng, Y. C.; Fleming, G. R. Two-Dimensional Electronic Spectroscopy of Molecular Aggregates. *Acc. Chem. Res.* **2009**, *42*, 1352−1363.
(21) Schlau-Cohen, G. S.; Dawlaty, J. M.; Fleming, G. R. Ultrafast Multidimensional Spectroscopy: Principles and Applications to Photosynthetic Systems. *IEEE J. Sel. Top. Quantum Electron.* **2012**, *18*, 283−295.
(22) Schlau-Cohen, G. S.; Ishizaki, A.; Fleming, G. R. Two-Dimensional Electronic Spectroscopy and Photosynthesis: Fundamentals and Applications to Photosynthetic Light-Harvesting. *Chem. Phys.* **2011**, *386*, 1−22.
(23) Jonas, D. M. Two-Dimensional Femtosecond Spectroscopy. *Annu. Rev. Phys. Chem.* **2003**, *54*, 425−463.
(24) Schlau-Cohen, G. S.; Calhoun, T. R.; Ginsberg, N. S.; Ballottari, M.; Bassi, R.; Fleming, G. R. Spectroscopic Elucidation of Uncoupled Transition Energies in the Major Photosynthetic Light-Harvesting Complex, LHCII. *Proc. Natl. Acad. Sci. U. S. A.* **2010**, *107*, 13276−13281.
(25) Read, E. L.; Schlau-Cohen, G. S.; Engel, G. S.; Wen, J. Z.; Blankenship, R. E.; Fleming, G. R. Visualization of Excitonic Structure in the Fenna-Matthews-Olson Photosynthetic Complex by Polarization-Dependent Two-Dimensional Electronic Spectroscopy. *Biophys. J.* **2008**, *95*, 847−856.
(26) Groot, M. L.; Yu, J.-Y.; Agarwal, R.; Norris, J. R.; Fleming, G. R. Three-Pulse Photon Echo Measurements on the Accessory Pigments in the Reaction Center of Rhodobacter sphaeroides. *J. Phys. Chem. B* **1998**, *102*, 5923−5931.
(27) Arnett, D. C.; Moser, C. C.; Dutton, P. L.; Scherer, N. F. The First Events in Photosynthesis: Electronic Coupling and Energy Transfer Dynamics in the Photosynthetic Reaction Center from Rhodobacter sphaeroides. *J. Phys. Chem. B* **1999**, *103*, 2014−2032.
(28) Jonas, D. M.; Lang, M. J.; Nagasawa, Y.; Joo, T.; Fleming, G. R. Pump-Probe Polarization Anisotropy Study of Femtosecond Energy Transfer within the Photosynthetic Reaction Center of Rhodobacter Sphaeroides R26. *J. Phys. Chem.* **1996**, *100*, 12660−12673.
(29) Pan, J.; Lin, S.; Woodbury, N. W. Bacteriochlorophyll Excited-State Quenching Pathways in Bacterial Reaction Centers with the Primary Donor Oxidized. *J. Phys. Chem. B* **2012**, *116*, 2014−2022.
(30) Huang, L. B.; Ponomarenko, N.; Wiederrecht, G. P.; Tiede, D. M. Cofactor-Specific Photochemical Function Resolved by Ultrafast Spectroscopy in Photosynthetic Reaction Center Crystals. *Proc. Natl. Acad. Sci. U. S. A.* **2012**, *109*, 4851−4856.
(31) Hochstrasser, R. M. Two-Dimensional Ir-Spectroscopy: Polarization Anisotropy Effects. *Chem. Phys.* **2001**, *266*, 273−284.
(32) Barron, L. D. *Molecular Light Scattering and Optical Activity*; Cambridge University Press: New York, 2004.
(33) Dreyer, J.; Moran, A. M.; Mukamel, S. Tensor Components in Three Pulse Vibrational Echoes of a Rigid Dipeptide. *Bull. Korean Chem. Soc.* **2003**, *24*, 1091−1096.
(34) Read, E. L.; Engel, G. S.; Calhoun, T. R.; Mancal, T.; Ahn, T. K.; Blankenship, R. E.; Fleming, G. R. Cross-Peak-Specific Two-Dimensional Electronic Spectroscopy. *Proc. Natl. Acad. Sci. U. S. A.* **2007**, *104*, 14203−14208.
(35) Jordanides, X. J.; Scholes, G. D.; Shapley, W. A. R., Jr.; Fleming, G. R. Electronic Couplings and Energy Transfer Dynamics in the Oxidized Primary Electron Donor of the Bacterial Reaction Center. *J. Phys. Chem. B* **2004**, *108*, 1753−1765.
(36) Brixner, T.; Stenger, J.; Vaswani, H. M.; Cho, M.; Blankenship, R. E.; Fleming, G. R. Two-Dimensional Spectroscopy of Electronic Couplings in Photosynthesis. *Nature* **2005**, *434*, 625−628.
(37) Ishizaki, A.; Calhoun, T. R.; Schlau-Cohen, G. S.; Fleming, G. R. Quantum Coherence and Its Interplay with Protein Environments in Photosynthetic Electronic Energy Transfer. *Phys. Chem. Chem. Phys.* **2010**, *12*, 7319−7337.
(38) Ishizaki, A.; Fleming, G. R. Unified Treatment of Quantum Coherent and Incoherent Hopping Dynamics in Electronic Energy Transfer: Reduced Hierarchy Equation Approach. *J. Chem. Phys.* **2009**, *130*, 234111−234110.
(39) May, V. Higher-Order Processes of Excitation Energy Transfer in Supramolecular Complexes: Liouville Space Analysis of Bridge Molecule Mediated Transfer and Direct Photon Exchange. *J. Chem. Phys.* **2008**, 129.
(40) Albinsson, B.; Martensson, J. Excitation Energy Transfer in Donor-Bridge-Acceptor Systems. *Phys. Chem. Chem. Phys.* **2010**, *12*, 7338−7351.
(41) Scholes, G. D. Long-Range Resonance Energy Transfer in Molecular Systems. *Annu. Rev. Phys. Chem.* **2003**, *54*, 57−87.
(42) deWinter, A.; Boxer, S. G. The Mechanism of Triplet Energy Transfer from the Special Pair to the Carotenoid in Bacterial Photosynthetic Reaction Centers. *J. Phys. Chem. B* **1999**, *103*, 8786−8789.
(43) Cogdell, R. J.; Frank, H. A. How Carotenoids Function in Photosynthetic Bacteria. *Biochim. Biophys. Acta* **1987**, *895*, 63−79.
(44) Timpmann, K.; Freiberg, A.; Sundstrom, V. Energy Trapping and Detrapping in the Photosynthetic Bacterium Rhodopseudomonas-Viridis - Transfer-to-Trap-Limited Dynamics. *Chem. Phys.* **1995**, *194*, 275−283.
(45) Bernhardt, K.; Trissl, H. W. Escape Probability and Trapping Mechanism in Purple Bacteria: Revisited. *Biochim. Biophys. Acta, Bioenerg.* **2000**, *1457*, 1−17.
(46) Amesz, J.; Neerken, S. Excitation Energy Trapping in Anoxygenic Photosynthetic Bacteria. *Photosynth. Res.* **2002**, *73*, 73−81.
(47) Sener, M. K.; Olsen, J. D.; Hunter, C. N.; Schulten, K. Atomic-Level Structural and Functional Model of a Bacterial Photosynthetic Membrane Vesicle. *Proc. Natl. Acad. Sci. U. S. A.* **2007**, *104*, 15723−15728.
(48) Cogdell, R. J.; Monger, T. G.; Parson, W. W. Carotenoid Triplet-States in Reaction Centers from Rhodopseudomonas-Sphaeroides and Rhodospirillum-Rubrum. *Biochim. Biophys. Acta* **1975**, *408*, 189−199.
(49) Brixner, T.; Mancal, T.; Stiopkin, I. V.; Fleming, G. R. Phase-Stabilized Two-Dimensional Electronic Spectroscopy. *J. Chem. Phys.* **2004**, *121*, 4221−4236.
(50) Lepetit, L.; Joffre, M. Two-Dimensional Nonlinear Optics Using Fourier-Transform Spectral Interferometry. *Opt. Lett.* **1996**, *21*, 564−566.
(51) Ernst, R. R.; Bodenhausen, G.; Wokaun, A. *Principles of Nuclear Magnetic Resonance in One and Two Dimensions*; Oxford University Press: New York, 1988.